CRYSTAL GROWTH & DESIGN

Subscriber access provided by TULANE UNIVERSITY

Article

A Functional 2D Coordination Polymer Exhibiting Luminescent Detection of Nitroaromatics

Zilong Tang, Hongjuan Chen, Yong Zhang, Baishu Zheng, Shaowei Zhang, and Peng Cheng

Cryst. Growth Des., **Just Accepted Manuscript** • DOI: 10.1021/acs.cgd.8b01640 • Publication Date (Web): 16 Jan 2019

Downloaded from http://pubs.acs.org on January 18, 2019

Just Accepted

“Just Accepted” manuscripts have been peer-reviewed and accepted for publication. They are posted online prior to technical editing, formatting for publication and author proofing. The American Chemical Society provides “Just Accepted” as a service to the research community to expedite the dissemination of scientific material as soon as possible after acceptance. “Just Accepted” manuscripts appear in full in PDF format accompanied by an HTML abstract. “Just Accepted” manuscripts have been fully peer reviewed, but should not be considered the official version of record. They are citable by the Digital Object Identifier (DOI®). “Just Accepted” is an optional service offered to authors. Therefore, the “Just Accepted” Web site may not include all articles that will be published in the journal. After a manuscript is technically edited and formatted, it will be removed from the “Just Accepted” Web site and published as an ASAP article. Note that technical editing may introduce minor changes to the manuscript text and/or graphics which could affect content, and all legal disclaimers and ethical guidelines that apply to the journal pertain. ACS cannot be held responsible for errors or consequences arising from the use of information contained in these “Just Accepted” manuscripts.

ACS Publications

is published by the American Chemical Society. 1155 Sixteenth Street N.W., Washington, DC 20036

Published by American Chemical Society. Copyright © American Chemical Society. However, no copyright claim is made to original U.S. Government works, or works produced by employees of any Commonwealth realm Crown government in the course of their duties.

A Functional 2D Coordination Polymer Exhibiting Luminescent Detection of Nitroaromatics

Published as part of a Crystal Growth and Design virtual special issue on Crystalline Functional Materials in Honor of Professor Xin-Tao Wu

Zilong Tang,[†] *Hongjuan Chen,*[†] *Yong Zhang,*[†] *Baishu Zheng,*[†] *Shaowei Zhang,*[*,†,‡,§] *and Peng Cheng*[*,‡]

[†]Key Laboratory of Theoretical Organic Chemistry and Functional Molecule of the Ministry of Education, Hunan Provincial Key Laboratory of Controllable Preparation and Functional Application of Fine Polymers, Hunan Provincial Key Laboratory of Advanced Materials for New Energy Storage and Conversion, School of Chemistry and Chemical Engineering, Hunan University of Science and Technology, Xiangtan, Hunan, 411201, China.

[‡]College of Chemistry, Key Laboratory of Advanced Energy Material Chemistry (MOE), Nankai University, Tianjin 300071, China.

[§]Henan Key Laboratory of Polyoxometalate Chemistry, College of Chemistry and Chemical Engineering, Henan University, Kaifeng 475004, China.

KEYWORDS: Coordination polymer; Crystal structure; Luminescent sensor; Nitroaromatics

ABSTRACT: A polyfluorinated-aromatic carboxylic acid has been designed and synthesized by the acylation reaction, tetrafluoro-bis-(3,5-dicarboxyphenyl)terephthalamide (H_4bdtfa), which assembled with Zn^{2+} ions in the mixed solvents of DMF, py and H_2O under solvothermal conditions to produce a 2D coordination polymer (CP), $\{[Zn_2(bdtfa)(py)_3(H_2O)]\cdot 2DMF\}_n$ (**1**), (py = pyridine, DMF = *N*,*N'*-dimethylmethanamide). The final structure has been carefully characterized by various methods including single-crystal X-ray diffraction, powder X-ray diffraction (PXRD), infrared (IR) spectrum, and thermogravimetric (TG) analysis. Two types of four-coordinated Zn^{2+} centers present a two-dimensional '**sql**'-type layer through $bdtfa^{4-}$ ligands, and the adjacent layers are connected through hydrogen bonds and $\pi\cdots\pi$ stacking interactions to produe a 3D supramolecular framework. Luminescent results reveal that CP **1** can be regarded as a highly sensitive sensor for detecting nitroaromatics based on the fluorescence quenching effect. Moreover, the reason for the luminescent response of CP **1** towards nitroaromatics has been investigated by theoretical calculation, which indicates that the quenching reason can be primarily due to the energy- and electron-transfer as well as electrostatic interaction between nitroaromatics and CP **1**.

INTRODUCTION

Nitroaromatic compounds, as one kind of important chemical raw material, have been used extensively in various areas including leather and rubber, pharmaceuticals, explosives and so on. however, the misuse of the nitroaromatic compounds could have a significant impact on the environment, human health, and public safety because of their high toxicity and hazard.[1-2] Although lots of instrument equipments have been developed to analyze nitroaromatic compounds highly sensitive and selective, they usually require tedious pretreatment process, high expenses, and cumbersome portability.[3-5] As a result, it is meaningful to investigate inexpensive and convenient probes with high selectivity and sensitivity to monitor nitroaromatic compounds.

On the other hand, coordination polymers (CPs) consist of metal ions/clusters and organic ligands, constitute an interdisciplinary field that has expanded rapidly in the past decade. The nearly limitless choices and combinations of organic linkers and metal centers allow to prepare various structures with interesting properties including but not limited to, gas storage and separation, catalysis, chemical sensing, as well as bioimaging and drug delivery.[3-20] In particular, luminescent CPs have recently bloomed out as promising candidates for sensing of numerous analytes because of their inherent advantages over other traditional molecular sensors, such as good crystallinity, defined crystal structure, high surface area and porosity, as well as adjustable and modifiable structure-induced luminescence performance.[3-5] More importantly, the porosity of CPs could enhance the probability of host-guest interactions by adsorbing and pre-enriching analytes, thus improving the detecting sensitivity and detection limit. In addition, the open metal sites and Lewis acidic and basic sites of organic linkers are readily available for CPs by post-synthetic modifications or pre-design of the structures, which may improve the detection selectivity. As a result, lots of luminescent CPs based sensors have been prepared and employed for detecting cations, anions, organic molecules, explosives, environmental toxins, pH, temperature, and biomolecules, and so on.[3-5,17-54]

In this contribution, we design and synthesize a new polyfluorinated-aromatic ligand, tetrafluoro-bis-(3,5-dicarboxyphenyl)terephthalamide (H_4bdtfa) (Scheme 1), containing four coordinated carboxylate groups and two functional amide groups by the acylation reaction of 2,3,5,6-tetrafluoroterephthalic acid and 5-aminoisophthalic acid, to assemble with Zn^{2+} to construct luminescent CPs for the following considerations: (i) the H_4bdtfa ligand could act as a diisophthalic acid linker separated by a tetrafluoro- terephthalamide spacer, the special orientation of isophthalate subunit is in favor of the isolation of porous structures, and the four carboxylate groups can allow to combine different metal ions to form multi-dimensional structures. (ii) H_4bdtfa could be completely or partially deprotonated to produce abundant acid-base-dependent anions varying pH values (bdtfa^{4-}, Hbdtfa^{3-}, H_2bdtfa^{2-}, and H_3bdtfa^{-}), and thus lead to various structures. Moreover, the deprotonated bdtfa^{4-}, Hbdtfa^{3-}, H_2bdtfa^{2-}, and H_3bdtfa^{-} as well as the high electronegativity fluorine atoms can serve as hydrogen bonds donors and acceptors, which are beneficial to generate supramolecular structures. (iii) Both tetrafluoro-terephthalamide and isophthalate motifs are typical π-conjugate systems, which are favorable to produce $\pi\cdots\pi$ stacking interactions, thereby enhance the stability of the framework. (iv) H_4bdtfa is electron-rich and π-conjugated ligand with good electron-transfer capability, which may improve the sensing ability through host-guest interactions because of hydrogen bonds and $\pi\cdots\pi$ interactions. Moreover, the d^{10} electronic configuration Zn^{2+} ion and π-conjugated ligands are usually applied to prepare fluorescent materials.

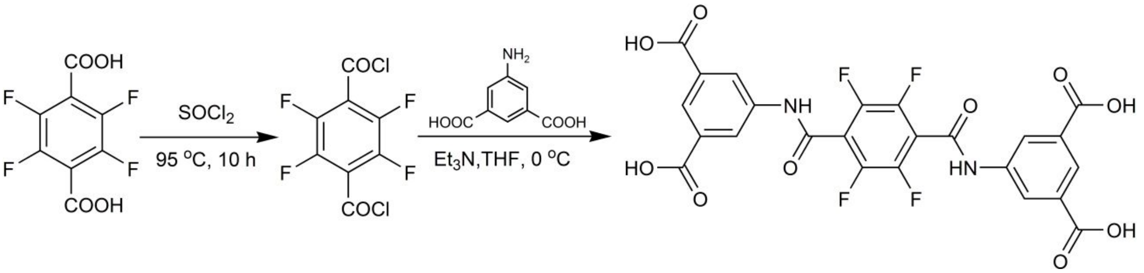

Scheme 1. The synthetic process of the H_4bdtfa ligand.

Based on the above considerations, we explored the reactions of H_4bdtfa and Zn^{2+} ions by regulating the rations of organic linkers and metal centers, reaction solvents, reaction temperature and pH value, *etc*. Herein, a 2D CP was obtained under solvothermal conditions, $\{[Zn_2(bdtfa)(py)_3(H_2O)]\cdot 2DMF\}_n$ (**1**), (DMF = *N*,*N'*-dimethylmethanamide, py = pyridine). The structure has been measured by the single-crystal X-ray diffraction, which further determined by PXRD, TG analysis and IR. The results demonstrate that the asymmetric skeleton of **1** has two kinds of Zn^{2+} centers, one $bdtfa^{4–}$ bridging ligand, three coordinated py molecules, one coordinated water molecule, and two uncombined DMF molecules. Two types of Zn^{2+} centers interconnected through $bdtfa^{4–}$ present a '**sql**'-type 2D layer, the neighbouring layers interact each other through hydrogen bonds and $\pi\cdots\pi$ interactions to from the 3D supramolecular architecture. The luminescent experiment of **1** has been carried out, which reveal that **1** could act as an excellent sensor to detect nitroaromatics on account of fluorescence quenching effect. Moreover, the reason for the luminescent response of **1** towards nitroaromatics has been investigated by theoretical calculation.

EXPERIMENTAL SECTION

General Methods and Materials. Unless otherwise specified, all reagents are commercially available and have been used directly. The ^{1}H-NMR and ^{13}C-NMR spectra are measured on a Bruker AV-II 500 MHz NMR spectrometer. Elemental analyse data are obtained from a Perkin-Elmer 2400-II CHNS/O analyzer. IR spectra are collected on a Nicolet 6700 spectrometer with KBr pellets in 4000–400 cm^{-1}. TG curve is acquired from a NETZSCH TG 209 Setaram apparatus with the heating rate of 10 $^{\circ}C\cdot min^{-1}$ under N_2 atmosphere. PXRD spectra are carried out on a Bruker D8 Advance instrument with Cu $K\alpha$ radiation (λ = 1.54056 Å). The luminescent experiments are finished on an F-4500 fluorescence spectrophotometer.

Synthesis of the H_4bdtfa ligand. 2,3,5,6-tetrafluoroterephthalic acid (2.0 g, 8.4 mmol) and 40.0 mL $SOCl_2$ were added in a 100 mL round-bottomed flask, the mixture was heated to 95 ˚C and stirred for 10 h. After cooling to room temperature, the excess $SOCl_2$ in the mixture was removed by reduced in the rotary evaporator to give the yellow oil. Then 40.0 mL THF was added into the above oil to harvest solution A. In another 500 mL round-bottomed flask, 5-aminoisophthalic acid (3.1 g, 17.0 mmol) and 180.0 mL THF were added and stirred at 0 ˚C, then solution A was dropwise added, and a yellow precipitate was produced almost immediately. Then 1.0 mL triethylamine was slowly added and stirred for 12 h at ambient temperature. The volume of THF was reduced in the rotary evaporator and then 80.0 mL 2 mol·L^{-1} HCl was added. The precipitate was filtrated and washed with DMF, H_2O and CH_3OH, and dried under vacuum to give a yellow powder (Scheme 1). Yield: *ca.* 77% (based on 2,3,5,6-tetrafluoroterephthalic acid). Anal. calcd (%) for $C_{24}H_{12}F_4N_2O_{10}$: C 51.08, H 2.14, N 4.96. Found: C 50.97, H 2.23, N 4.88. ^{1}H-NMR (DMSO-d^6, 500 MHz, δ/ppm): 13.39 (4H, COOH), 11.61 (2H, ArH), 8.55 (4H, ArH), 8.31 (2H, CONH) (Figure S1); ^{13}C-NMR (DMSO-d^6, 125 MHz, δ/ppm): 166.14, 155.65, 143.63, 141.64, 141.54, 138.38, 132.14, 126.01, 123.99, 117.90 (Figure S2). IR (KBr pellets): 3429 (br), 1706 (s), 1677 (s), 1624 (m), 1582 (s), 1479 (s), 1433 (m), 1403 (m), 1350 (m), 1267 (m), 1235 (m), 994 (s), 948 (w), 782 (w), 759 (w), 679 (m) cm^{-1} (Figure S3).

Synthesis of {[Zn_2(bdtfa)(py)$_3$(H_2O)]·2DMF}$_n$ (1). $Zn(NO_3)_2\cdot6H_2O$ (0.0592 g, 0.20 mmol) and H_4bdtfa (0.0282 g, 0.05 mmol) were added in a 5 mL mixed solvents (H_2O:py:DMF = 1:1:8) in a 20 mL vial. Colorless block crystals were obtained after being placed in an oven at 80 ˚C for three days. Yield: *ca.* 62% (based on H_4bdtfa). Anal. calcd (%) for $C_{45}H_{39}F_4N_7O_{13}Zn_2$: C 49.47, H 3.60, N 8.97. Found: C 49.59, H 3.68, N 9.03. IR (KBr pellets): 3447 (br), 1686 (m), 1653 (s), 1622 (m), 1561 (m), 1474 (w), 1449 (m), 1434 (w), 1384 (m), 1332 (m), 1202 (m), 1107 (m), 1070 (m), 1046 (m), 996 (m), 781 (m), 761 (m), 734 (m), 697 (m) cm^{-1} (Figure S3).

X-ray Crystallography. The crystal **1** was measured on a Bruker Apex-II CCD diffractometer with monochromatic Mo $K\alpha$ radiation (λ = 0.71073 Å) at 296(2) K, Absorption and scaling correction were undertaken with SADABS program, and the direct method was used to resolve the crystal structure, except for hydrogen atoms, other atoms were refined by the full-matrix least-square procedure employing the free Olex2 program embedded with SHELXL-2016.[55-56] The refinement details for CP **1** have been explained in the .cif document, and the crystallographic data and refinement parameters for **1** have been summarized in Table 1 (CCDC no. 1852625).

Table 1. Crystallographic Data and Refinement Parameters for **1**.

	1
formula	$C_{45}H_{39}F_4N_7O_{13}Zn_2$
*M*r (g mol^{-1})	1092.57
T (K)	296(2)
Cryst syst	Triclinic
space group	*P*-1
a (Å)	12.5194(14)
b (Å)	14.5007(16)
c (Å)	16.5672(19)
α (°)	80.405(2)
β (°)	70.320(2)
γ (°)	69.843(1)
V (Å^3)	2654.1(5)
Z	2
Dc (g cm^{-3})	1.367
μ (mm^{-1})	0.982
R_{int}	0.0482
limiting indices	$-14 \leq h \leq 14$ $-17 \leq k \leq 17$ $-19 \leq l \leq 19$

reflns collected	9300
indep reflns	6567
params	692
GOF on F^2	1.057
$R_1{}^a$, $wR_2{}^b$ [$I>2\sigma(I)$]	0.0715 0.0996
$R_1{}^a$, $wR_2{}^b$ [all data]	0.1915 0.2154
$\Delta\rho_{max}/\Delta\rho_{min}$ (e Å^{-3})	0.821/-0.635

^{a} $R_1 = \Sigma||F_o|-|F_c||/\Sigma|F_o|$; ^{b} $wR_2 = \{\Sigma[w(F_o{}^2-F_c{}^2)^2]/\Sigma[w(F_o{}^2)^2]\}^{1/2}$.

Luminescent experiments. Nitrobenzene (NB) was diluted 100 times with DMF before used. For other nitroaromatic compounds including 2,4,6-trinitrophenol (PA), 2,4-dinitophenol (BNP), *o*-nitroaniline (oNA), *o*-nitrophenol (oNP), *p*-nitroaniline (pNA), *p*-nitrophenol (pNP), *m*-nitroaniline (mNA), and *m*-nitrophenol (mNP), the corresponding 10^{-2} mol·L^{-1} analyte solutions were prepared with DMF, respectively. The concentration-dependent intensity test was executed as shown below: soaking 3 mg CP **1** in 2.0 mL DMF to disperse evenly with ultrasound, then adding the corresponding 10^{-2} mol·L^{-1} solutions containing different nitroaromatic compounds in the above suspension.

RESULTS AND DISCUSSION

Structural Descriptions. The as-synthesized bulky crystals **1** has a high phase purity, which were proved by comparing the simulated PXRD pattern with the experimental one (Figure S4). Moreover, when immersing **1** in DMF for three days, the experimental PXRD pattern is also agreement with the simulated one (Figure S4), indicating the structure of **1** can maintain in DMF at least three days.

Crystal structure results of **1** display that it belongs to the triclinic system with the space group *P*-1. In the asymmetric structure (Figure 1a), there are two Zn^{2+} centers, one bdtfa^{4-} ligand, three coordinated py molecules, one coordinated water, and two unbounded DMF molecules, and the formula as follows, $\{[Zn_2(bdtfa)(py)_3(H_2O)]\cdot 2DMF\}_n$ (**1**). Both two independent Zn^{2+} ions adopt the four-coordinated tetrahedral geometry. Zn1 is defined by two carboxyl O atoms of two $bdtfa^{4-}$ through the bridging mode, one water molecule [Zn1-O: 1.941(4) – 1.976(3) Å], and one py molecule [Zn1-N: 2.030(5) Å]. Whereas Zn2 center is surrounded by two carboxyl O atoms of two $bdtfa^{4-}$ by the bridging mode [Zn2-O: 2.028(4) – 2.063(5) Å], and two py molecules [Zn2-N: 2.061(5) – 2.068(6) Å] (The selected bond lengths and angles, see Table S1 and S2). It is important to note that the $bdtfa^{4-}$ ligand also exhibits two kinds of coordinated orientations because the amide bonds can rotate freely, resulting into two different angles between the two sides of benzene rings and the tetrafluoro-benzene ring (Figure 1b, c). Neighboring Zn^{2+} ions are bridged by $bdtfa^{4-}$ to produce a 2D layer containing two kinds of rectangular channels in the *bc* plane, in which are occupied by the free DMF molecules (Figure 1d). To describe the 2D architechture of **1** more clearly, the freely available program TOPOS 5.0[57] is used to analyze the topological structure. If every Zn^{2+} ion is regarded as a node and each $bdtfa^{4-}$ serves as a linker, CP **1** could simplify as the 4-connected '**sql**'-type topological structure, and the corresponding Schläfli symbol is $\{4^4\cdot 6^2\}$ (Figure 1e).

It is worth noting that many C, N and O atoms, as well as the high electronegativity F atoms in **1** may be as hydrogen bonds donors and acceptors to produce supramolecular architecture. Furthermore, the offset arrangements of benzene and pyridine in **1** is opposite to the edge-to-face and face-to-face, which could form strong $\pi\cdots\pi$ stacking interactions. As a result, the neighbouring layers could stack to give a supramolecular architecture (Figure 1f) by $\pi\cdots\pi$ stacking interactions as well as inter- and intramolecular hydrogen bonds (Table S3).

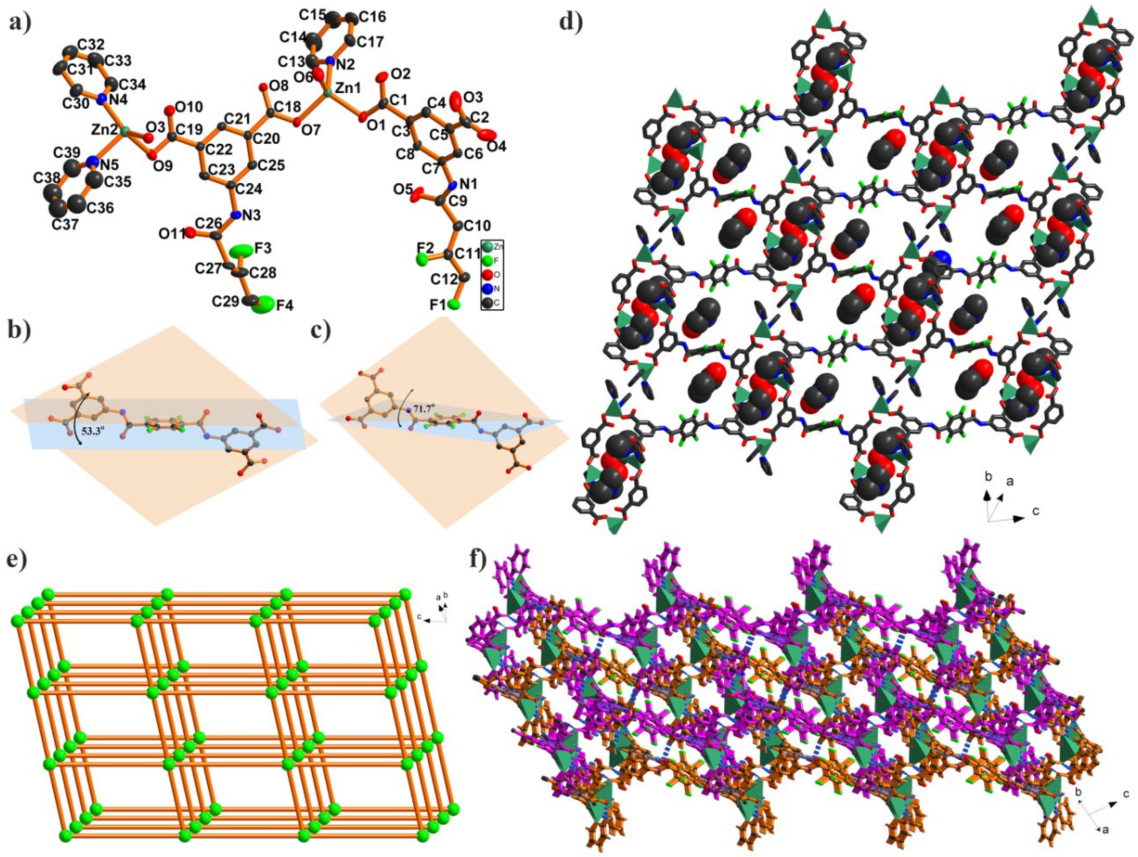

Figure 1. a) The thermal ellipsoids plot representation of the asymmetric skeleton of **1**, H and isolated DMF molecules are not shown for clarity; b) and c) The two kinds of coordinated orientations of bdtfa^{4-} ligands in **1**; d) The 2D network of **1**, in which are occupied by isolated DMF molecules presented as space-filling mode; e) The simplified 4-connected '**sql**'-type topological structure of **1**. f) The 3D supramolecular structure of **1**.

Luminescent properties. CPs constructed from d^{10} electronic configuration metal centers and π-conjugated organic ligands are generally chosen to evaluate their luminescent properties.[58-59] In the case of **1**, H_4bdtfa is π-conjugated and electron-rich ligand with good electron-transfer ability, and is coordinate with d^{10} electronic configuration Zn^{2+} ions, which encourages us to explore its luminescent performance. Therefore, we measure the solid state emission spectrum of **1** at ambient temperature, and it shows one obvious emission band at *ca.* 458 nm when excited at

356 nm (Figure S5). To explore the origin of the luminescent emission of CP **1**, the solid state luminescence spectrum of the free H_4bdtfa ligand has been also carried out at the same conditions (Figure S5). The similar emission band at *ca.* 388 nm is presented by the H_4bdtfa ligand, which may be ascribed to the intra-ligand emission state of $\pi^* \rightarrow \pi$ transition.[58] By comparing the emission spectra of **1** and H_4bdtfa, it can be seen that the emission signal of **1** is neither ligand-to-metal charge transfer (LMCT) nor metal-to-ligand charge transfer (MLCT), which may be mainly ascribed to the d^{10} configuration Zn^{2+} center is relatively difficult to reduce or oxidize, and this phenomenon is usually encountered in previous reports.[58] Thus, the luminescent emission of **1** could be mainly due to the intra-ligand charge transfer transition. Moreover, the luminescence intensity of **1** is slightly enhanced, which can be explained that the ligand binds to mental center to increase the rigidity compared with the free H_4bdtfa ligand, therefore decreasing the energy loss of radiation-less decay. In addition, the luminescent emission spectrum of **1** is distinctly red-shifted compared with the free H_4bdtfa ligand, manifesting the existence of coordination interactions among the H_4bdtfa ligand and Zn^{2+} centers.[59]

Previous results suggest that the energy and electron could transfer from electron-donating complex to high electron-withdrawing nitro-compound under photo-excitation, which usually result in the fluorescence weaken or completely quenched.[52-54,59] From the structural descriptions of **1**, the $\pi\cdots\pi$ interactions and hydrogen bonds could strengthen the interactions between analytes and target compound, and thus improve the sensing ability. Therefore, the electron-withdrawing nitroaromatic compounds containing NB, PA, BNP, oNA, oNP, mNA, mNP, pNA, and pNP are chosen to assess the luminescent sensitivity of **1**.

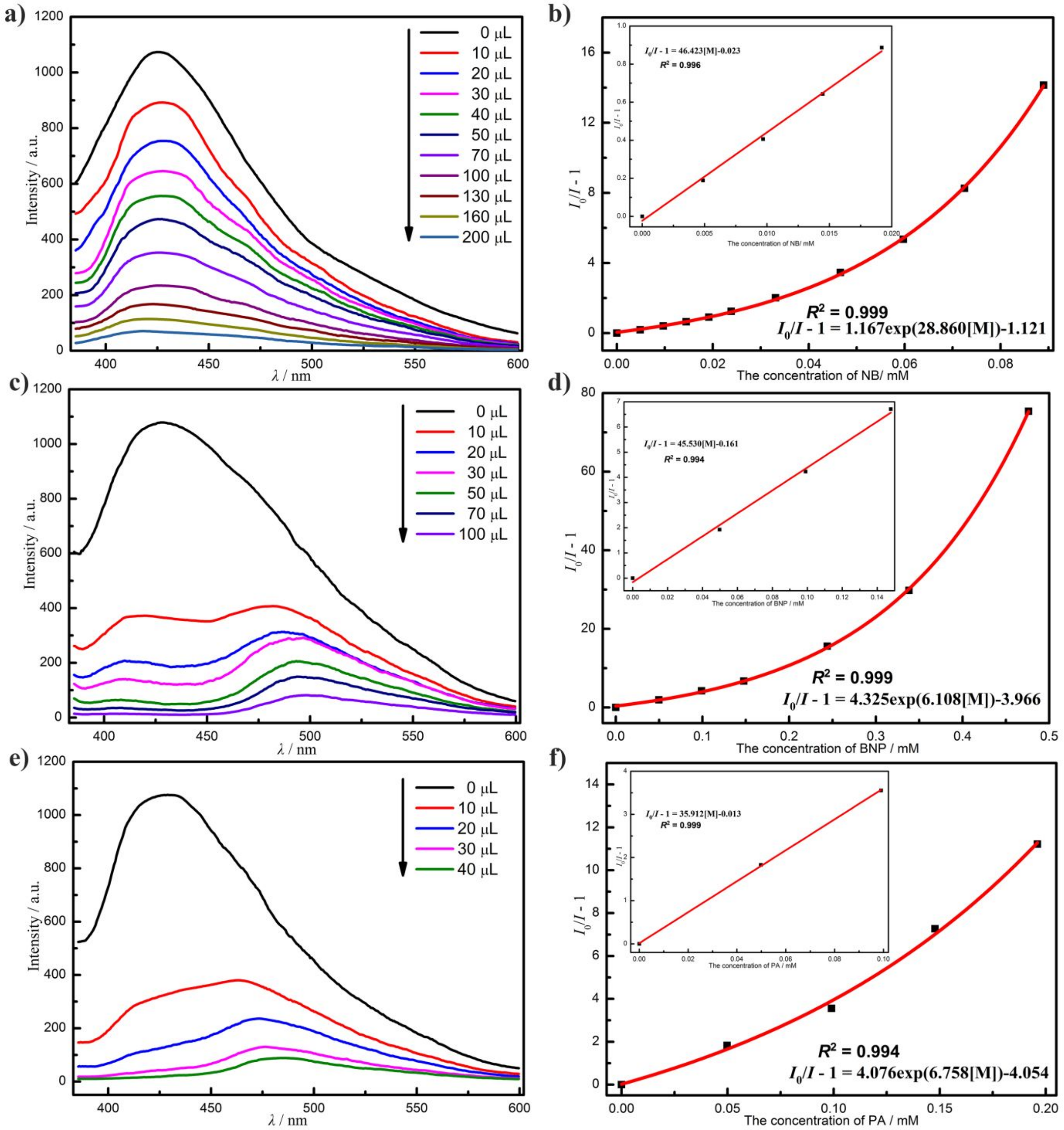

Figure 2. The concentrations-dependent emission spectra (λ_{ex} = 345 nm) and Stern-Volmer plots of **1** in DMF towards various concentrations of nitroaromatic compounds, NB (a and b), BNP (c and d), and PA (e and f), respectively.

The luminescent experiments of concentration-dependent intensity are executed by slowly adding different amount of nitroaromatic compounds into the well-dispersed suspensions of **1**, and the concentration-dependent intensity for NB is selected as a representative of the specific description. The emission intensity decreases as gradually adding NB, almost quenched when the amount of NB attains 200 μL (1091 ppm) (Figure 2a), and the quenching efficiency is 93.4%. The quenching effciency of NB can be assessed by employing the Stern-Volmer (S-V) equation, $I_0/I - 1 = K_{SV}[M]$,[59] in which I_0 and I are the emission intensities of maximum emission band before and after the addition of NB, respectively, [M] represents the molar concentration of the NB analyte (mM), and K_{SV} is the S-V constant (M^{-1}). The maximum emission intensities at *ca.* 425 nm versus the concentration of NB analyte are plotted and presented in Figure 2b. When the concentration of NB is lower than 0.02 mM, the S-V curve is nearly linear, and the detection limit can be calculated to be 9.15×10^{-7} $mol \cdot L^{-1}$ by the equation $3\sigma/k$, in which σ is the standard deviation of luminescent intensities of 10 field blanks, k is the slope.[60] However, when concentration of NB is higher than 0.02 mM, the S-V curve is apparent deviation from linearity, which may mainly due to the reason that the presence of self-absorption and/or the dynamic quenching and static quenching resulted from the energy-transfer process.[52-54] In order to assess the whole concentration, we employ an exponential S-V formula, $I_0/I = a*\exp(k[M]) + b$,[28] in which I_0 and I are the maximum emission intensities before and after adding NB, respectively, [M] represents the concentration of NB(mM), a, b, and k are constants. The results demonstrate that the whole range could match well with the equation $I_0/I = 1.167*\exp(28.860[M]) - 1.121$ (Figure 2b), and the quenching constant of NB is 3.368×10^4 $L \cdot mol^{-1}$ calculated from the fitted values of a and k.

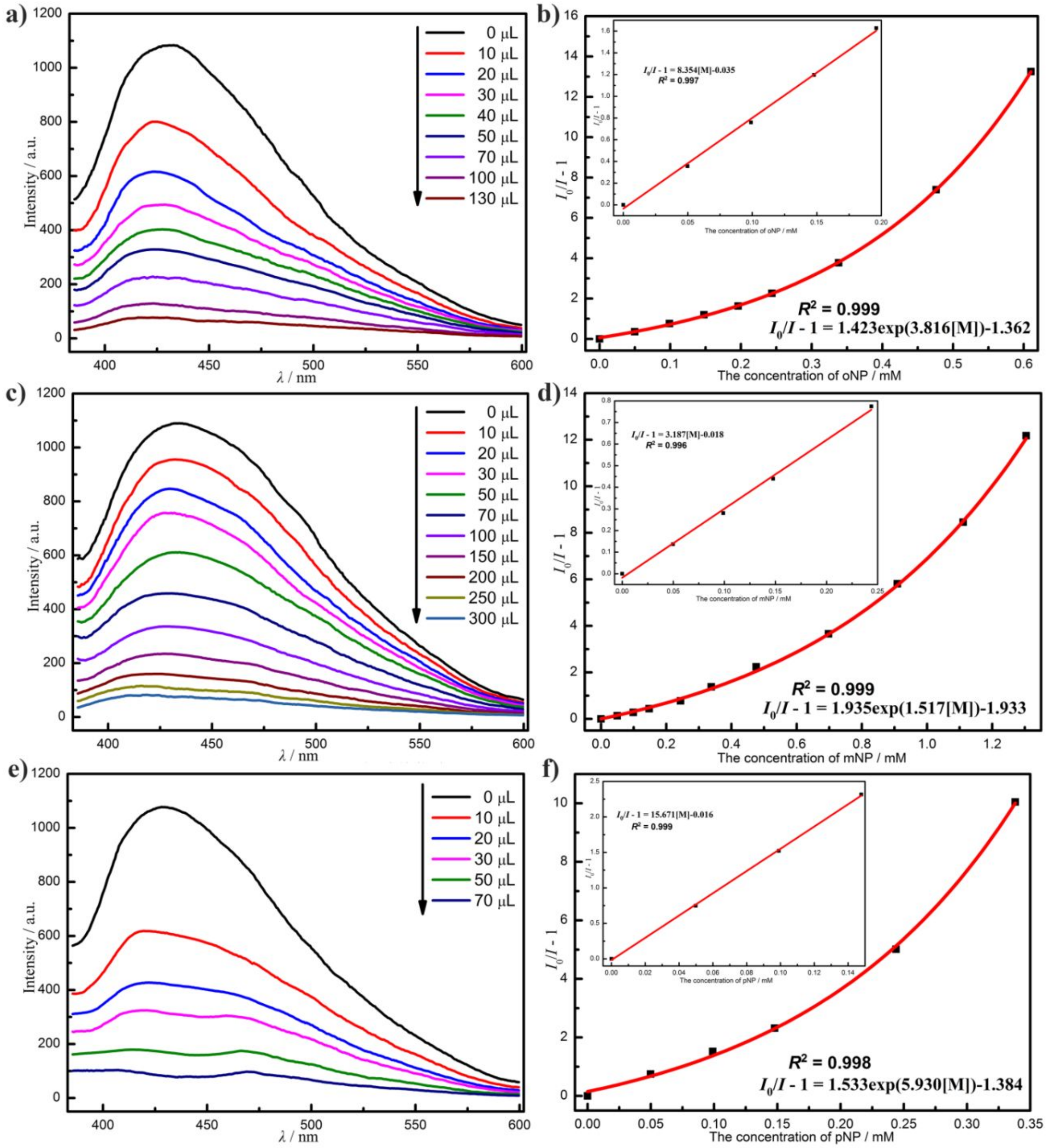

Figure 3. The concentrations-dependent emission spectra (λ_{ex} = 345 nm) and Stern-Volmer plots of **1** in DMF toward various concentrations of nitroaromatic compounds, oNP (a and b), mNP (c and d), and pNP (e and f), respectively.

Analogously, other nitroaromatic compounds have been analyzed by the same methods (Figure 2c-f, 3, and 4), the quenching efficiencies are 98.7% (100 μL), 91.8% (40 μL), 93.0% (130 μL), 92.5% (300 μL), 90.9% (70 μL), 91.9% (500 μL), 93.0% (800 μL), and 92.7% (100 μL) for

BNP, PA, oNP, mNP, pNP, oNA mNA and pNA, and the detection limits can be calculated to be 1.61×10^{-7}, 1.86×10^{-7}, 1.07×10^{-6}, 5.07×10^{-5}, 2.60×10^{-6}, 3.13×10^{-5}, 1.52×10^{-5}, and 8.55×10^{-6} mol·L^{-1}, respectively. Furthermore, the quenching constants obtained from a and k values by fitting the exponential S-V equation are 2.642×10^{4}, 2.755×10^{4}, 5.430×10^{3}, 2.935×10^{3}, 9.091×10^{3}, 2.018×10^{3}, 1.896×10^{3}, and 1.694×10^{4} L·mol^{-1}, respectively (Figure 2c-f, 3, and 4), which are comparatively high among the documented CP-based sensors for probing nitroaromatic compounds (Table 2).[52-54] Additionally, it is important to note that PA exhibits the largest quenching efficiency of 87.9% at the same concentration (30 μL) in the selected nitroaromatic compounds (87.0% for BNP, 72.6% for pNA, 70.0% for pNP, 54.5% for oNP, 31.6% for oNA, 30.5% for mNP, and 25.5% for mNA, respecitvely), namely, **1** could be employed as an excellent sensor for detecting PA.

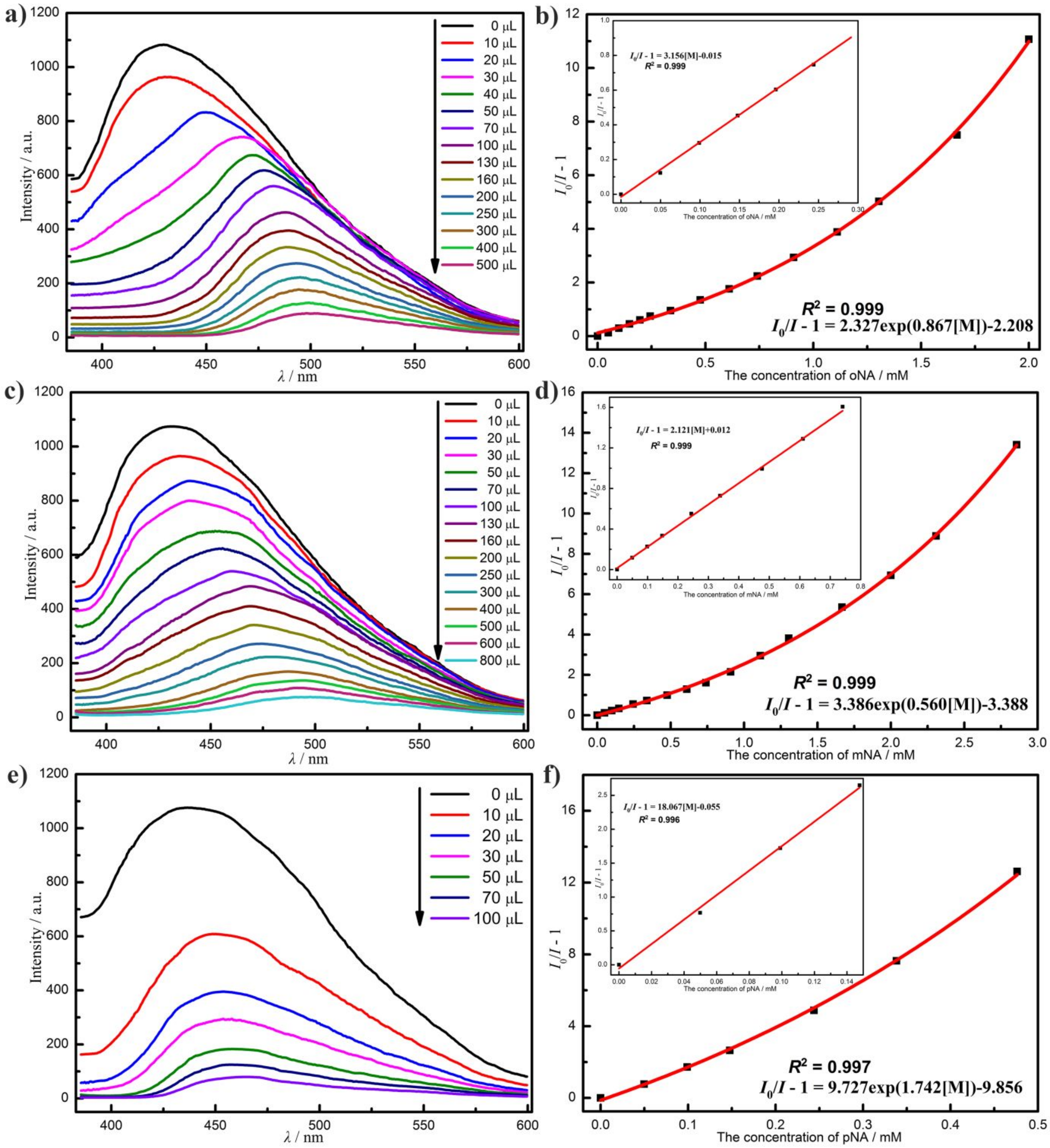

Figure 4. The concentrations-dependent emission spectra (λ_{ex} = 345 nm) and Stern-Volmer plots of **1** in DMF toward various concentrations of nitroaromatic compounds, oNA (a and b), mNA (c and d), and pNA (e and f), respectively.

Table 2. Selected CP-based sensors for the detection of nitroaromatics.

Sensing Material[a]	Target	Quenching constant (K_{sv}, $L\cdot mol^{-1}$)	Limit of detection ($mol\cdot L^{-1}$)
$[Cd(ppvppa)(1,4\text{-}NDC)]_n$[33]	BNP	1.18×10^2	-
	pNP	15	-
$[Me_2NH_2]_4[Zn_6(qptc)_3(trz)_4]\cdot 6H_2O$[34]	PA	2.08×10^6	-
$[Cd(ndc)(L^1)]_2\cdot H_2O$[35]	PA	3.7×10^4	-
$[Tb(L^7)(HL^7)(H_2O)_2]_n$[36]	BNP	7.75×10^3	1.62×10^{-2}
$[Eu_2(H_2L^6)_3(H_2O)_2]\cdot 21H_2O$[37]	NB	2.5×10^4	-
	pNP	4.6×10^3	-
$\{(Me_2NH_2)_{10}[Zn_6(TDPAT)_4(\mu_3\text{-}O)_2Zn_3]\cdot G_x\}_n$[38]	BNP	5.11×10^4	2.87×10^{-6}
	pNA	2.28×10^4	1.75×10^{-7}
$[Zn(bpba)(NO_3)]$[39]	oNA	1.20×10^4	-
	mNA	3.1×10^2	-
	NB	1.73×10^3	-
$[\{Cd_2(4\text{-}tp\text{-}3\text{-}lad)(1,4\text{-}BDC)_2\}\cdot 2MeCN]_n$[40]	BNP	5.3×10^4	2.28×10^{-7}
$[\{Cd(ppene)(1,4\text{-}BDC)\}\cdot MeCN]_n$[40]	BNP	3.3×10^4	1.03×10^{-6}
$Zr_6O_4(OH)_4(L^2)_6$[41]	PA	2.9×10^4	-
$Zn_2(TZBPDC)(\mu_3\text{-}OH)(H_2O)_2$[42]	PA	4.9×10^4	2.78×10^{-4}
$[Mg_2Zn_2(OH)_2(1,4\text{-}NDC)_3(H_2O)_2]\cdot 6H_2O$[43]	oNP	9.4×10^3	-
	PA	1.8×10^4	-
$Zr_6O_4(OH)_4(L^4)_6$[44]	PA	5.8×10^4	-
$[Zn_3(TPT)_2(DMF)_2]\cdot 0.5HNMe_2$[45]	PA	6.39×10^4	-
$NH_2Me_2\cdot[Zn(TPT)]\cdot DMF$[45]	PA	7.18×10^4	-
$Tb(L^5)_2$[46]	PA	3.8×10^4	5.0×10^{-8}
$Zr_6O_4(OH)_8(H_2O)_4(TTNA)_{8/3}$[47]	pNP	4.7×10^4	-

	PA	5.1×10^{5}	-
	NB	5.7×10^{4}	-
$[Zn_8(ad)_4(BPDC)_6O\cdot 2Me_2NH_2]\cdot G$[48]	PA	4.6×10^{4}	1.29×10^{-8}
$[Zn_2(tptc)(apy)(H_2O)]\cdot H_2O$[49]	NB	4.86×10^{3}	-
$[Zn_4(DMF)(Ur)_2(2,6\text{-}NDC)_4]$[50]	PA	1.08×10^{3}	-
$\{[Zn_2(L^3)(5\text{-}AIP)_2]\cdot 3H_2O\}_n$[51]	PA	4.19×10^{4}	-
	pNP	2.93×10^{4}	-
$Rh_6G@\{(Me_2NH_2^+)_5[Na_{31}(TATB)_{12}](DMF)_{30}(H_2O)_{92}\}_n$[52]	PA	4.1×10^{4}	-
$Pb_3O_2(L^8)$[53]	PA	5.98×10^{4}	1.58×10^{-6}
	NB	3.37×10^{4}	9.15×10^{-7}
	pNP	9.09×10^{3}	2.60×10^{-6}
$\{[Zn_2(bdtfa)(py)_3(H_2O)]\cdot 2DMF\}_n$ (**This work**)	BNP	2.64×10^{4}	1.61×10^{-7}
	PA	2.76×10^{4}	1.86×10^{-7}
	pNA	1.69×10^{4}	8.55×10^{-6}

---

[a] ppvppa = N-(pyridin-2-yl)-N-(4-(2-(pyridin-4-yl)vinyl)phenyl)pyridin-2-amine; trz = 1,2,4-triazole; 1,4-H_2NDC = 1,4-naphthalenedicarboxylic acid; H_4qptc = terphenyl-2,5,2′5′-tetracarboxylic acid; H_4L^6 = α-hydroxyphosphonic acid; L^1 = 4-amino-3,5-bis(4-imidazol-1-ylphenyl)-1,2,4-triazole; H_2L^7 = 5-(imidazol-1-yl)isophthalic acid; H_6TDPAT = 2,4,6-tris(3,5-dicarboxylphenylamino)-1,3,5-triazine; Hbpba = 4-(bis(4-(pyridin-4-yl)phenyl)amino)benzoic acid; 4-tp-3-lad = 2,3,5,6-tetra(pyridin-4-yl)-bicyclo[2.2.0]hexane; 1,4-H_2BDC = benzene-1,4-dicarboxylic acid; ppene = 4-pyrpoly-2-ene; H_2L^2 = 2-phenylpyridine-5,4'-dicarboxylic acid; $H_3TZBPDC$ = 4'-(1Htetrazol-5-yl)-[1,1'-biphenyl]-3,5-dicarboxylic acid; apy = aminopyridine; L^5 = 3-bis(3-carboxyphenyl)imidazolium; L^4 = 2'-amino-[1,1':4',1''-terphenyl]-4,4''-dicarboxylate; ad = adenine; H_3TPT = p-terphenyl-3,4'',5-tricarboxylic acid; H_3TTNA = 6,6',6''-(2,4,6-trimethylbenzene-1,3,5-triyl)tris(2-naphthoic acid; BPDC= biphenyl dicarboxylic acid; H_4tptc = terphenyl-3,3″,5,5″-tetracarboxylic acid; L^3 = 3-pyridin-3-yl-N-[5-(3-pyridin-3-yl-acryloylamino)-naphthalen-1-yl]-acrylamide; Ur = urotropin; H_2AIP = 5-amino isophthalic acid; TATB = 4,4',4''-(1,3,5-triazine-2,4,6-triyl)tris-benzoate; H_2L^8 = 4-(1H-tetrazol-5-yl)phenol; H_2ndc = 2,6-Naphthalenedicarboxylic acid.

In order to explore the reason for the fluorescence response of selected nitroaromatics, the response reason of **1** towards selected nitroaromatics has been investigated. First, the quenching probability caused by the structural breakage of **1** could be readily ruled out from PXRD experiments and IR spectra (Figure S4 and S6). Considering that the luminescent signal of **1** primarily comes from the intra-ligand charge transfer transition of the H_4bdtfa ligand. Therefore, the molecular orbitals of **1** are approximately computed with the H_4bdtfa ligand. The energy for highest occupied molecular orbital (HOMO) and lowest unoccupied molecular orbital (LUMO) of selected nitroaromatic compounds and H_4bdtfa ligand are calculated by the density functional theory at the B3LYP level (Figure 5).[52,59] The results suggest that the LUMO energy of the selective nitroaromatic compounds is smaller, the quenching potency is larger. The quenching potency of PA is highest among selected nitroaromatic compounds, which may be due to that the excited state electrons are most easily transferred from the conduction bands of H_4bdtfa to the LUMO orbital of PA since the lowest LUMO energy, However, the order of quenching constants of selected nitroaromatic compounds is not completely consistent with the energy of LUMO orbitals, manifesting the electron-transfer may be not the only factor of the luminescent response. The electrostatic interactions and/or energy transfer may be other possible reasons and be responsible for the luminescent response,[52-54,59] which is also supported by the exponential S-V curves. Indeed, many C, N, O and high electronegativity F atoms coexist in **1**, which can serve as hydrogen bonds acceptors and donors to increase the interactions between nitroaromatic compounds and CP **1**. Furthermore, the $\pi\cdots\pi$ stacking interactions in **1** also interact with nitroaromatis through the host-guest interactions. Consequently, the electron transfer and electrostatic interactions as well as energy-transfer can easily happen between nitroaromatic compounds and the framework of **1**, leading to the luminescent intensity weaken or even quenching.

In addition, the possible reason that PA has the largest quenching constant among the selected nitroaromatics can attribute to the following two aspects: firstly, the energy of LUMO for PA is lowest, which permits electron and energy-transfer from the framework of **1** to PA molecules is easiest and make the luminescent response most obvious.[59] On the other hand, the PA molecule possessing more -OH and -NO_2 groups could participate in the formation of hydrogen bonds with **1** stronger than other nitroaromatic compounds, the host-guest interaction between **1** and PA may be stronger, therefore the electrostatic interaction can take place more easily.

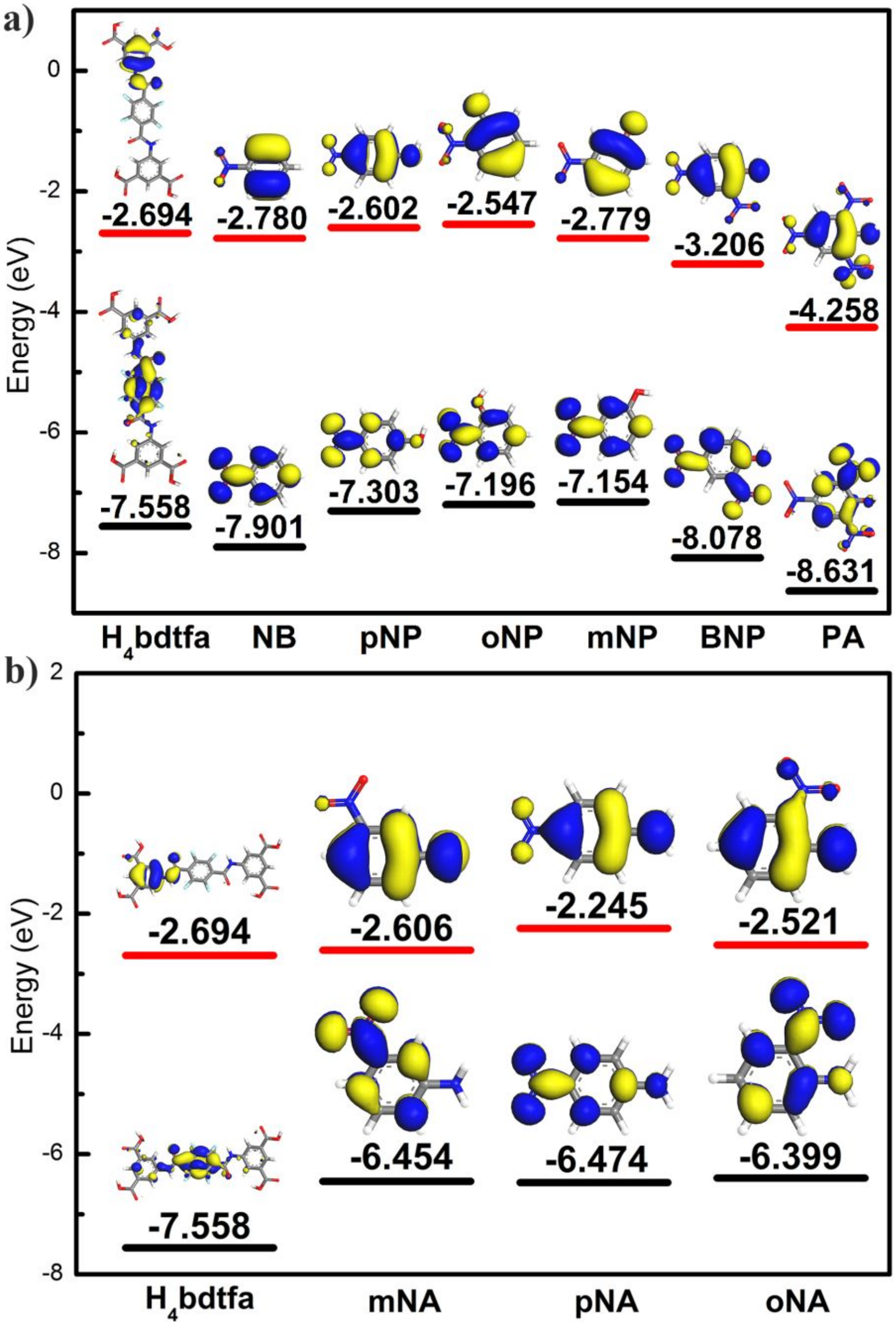

Figure 5. a) and b) The energy of HOMO and LUMO for selected nitroaromatics and H_4bdtfa.

CONCLUSIONS

In conclusion, a new polyfluorinated-aromatic carboxylic acid ligand was designed and prepared by the typical acylation reaction, which was further employed to react with Zn^{2+} ions to construct a 2D CP under the solvothermal conditions. The crystal structure demonstrates that two kinds of tetrahedral Zn^{2+} centers are bridged through $bdtfa^{4-}$ to produce a 2D '**sql**' topological structure, which further generate a 3D supramolecular architecture by $\pi\cdots\pi$ interactions and hydrogen bonds. Importantly, CP **1** can be regarded as a highly sensitive probe for detecting nitroaromatic compounds. Furthermore, the luminescent response of **1** towards nitroaromatic compounds has been preliminarily investigated by the theoretical calculation, and the reason could be primarily ascribed to energy- and electron-transfer and electrostatic interaction between nitroaromatic compounds and CP **1**.

ASSOCIATED CONTENT

Supporting Information

IR spectra, PXRD patterns, TG analysis and TG curve, and the solid-state emission spectra of **1** and the free H_4bdtfa ligand, as well as the information of bond lengths and angles of **1**. This material is available free of charge via the Internet at http://pubs.acs.org.

AUTHOR INFORMATION

Corresponding Author

*E-mail: swzhang@hnust.edu.cn (S.Z.); pcheng@nankai.edu.cn (P.C.).

Notes

The authors declare no competing financial interest.

ACKNOWLEDGMENT

This work was supported by the National Natural Science Foundation of China (21601058 and 21771112), 111 project (B12015), the Hunan Provincial Natural Science Foundation of China (2018JJ3146), the Open Research Fund of Henan Key Laboratory of Polyoxometalate Chemistry (HNPOMKF1602), and Hunan University of Science and Technology (E51677, STZ2018007, 201810534039 and CX2018B672).

REFERENCES

(1) Nagarkar, S. S.; Desai, A. V.; Ghosh, S. K. Engineering metal-organic frameworks for aqueous phase 2,4,6-trinitrophenol (TNP) sensing. *CrystEngComm* **2016,** *18*, 2994-3007.

(2) Zhang, L.; Kang, Z.; Xin, X.; Sun, D. Metal-organic frameworks based luminescent materials for nitroaromatics sensing. *CrystEngComm* **2016,** *18*, 193-206.

(3) Lustig, W. P.; Mukherjee, S.; Rudd, N. D.; Desai, A. V.; Li, J.; Ghosh, S. K. Metal-organic frameworks: functional luminescent and photonic materials for sensing applications. *Chem. Soc. Rev.* **2017,** *46*, 3242-3285.

(4) Zhang, Y.; Yuan, S.; Day, G.; Wang, X.; Yang, X.; Zhou, H.-C. Luminescent sensors based on metal-organic frameworks. *Coord. Chem. Rev.* **2018,** *354*, 28-45.

(5) Cui, Y.; Yue, Y.; Qian, G.; Chen, B. Luminescent Functional Metal-Organic Frameworks. *Chem. Rev.* **2011,** *112*, 1126-1162.

(6) Lin, Z.-J.; Lü, J.; Hong, M.; Cao, R. Metal–organic frameworks based on flexible ligands (FL-MOFs): structures and applications. *Chem. Soc. Rev.* **2014,** *43*, 5867-5895.

(7) Zhang, S.; Shi, W.; Cheng, P. The coordination chemistry of N-heterocyclic carboxylic acid: A comparison of the coordination polymers constructed by 4,5-imidazoledicarboxylic acid and 1H-1,2,3-triazole-4,5-dicarboxylic acid. *Coord. Chem. Rev.* **2017,** *352*, 108-150.

(8) Huang, Y.-B.; Liang, J.; Wang, X.-S.; Cao, R. Multifunctional metal–organic framework catalysts: synergistic catalysis and tandem reactions. *Chem. Soc. Rev.* **2017,** *46*, 126-157.

(9) Wang, Z.; Zheng, B.; Liu, H.; Lin, X.; Yu, X.; Yi, P.; Yun, R. High-Capacity Gas Storage by a Microporous Oxalamide- Functionalized NbO-Type Metal-Organic Framework. *Cryst. Growth Des.* **2013,** *13*, 5001-5006.

(10) Zhao, X.; Zhang, S.; Yan, J.; Li, L.; Wu, G.; Shi, W.; Yang, G.; Guan, N.; Cheng, P. Polyoxometalate-Based Metal-Organic Frameworks as Visible-Light-Induced Photocatalysts. *Inorg. Chem.* **2018,** *57*, 5030-5037.

(11) Zhang, S.; Cheng, P. Coordination-Cluster-Based Molecular Magnetic Refrigerants. *Chem. Rec.* **2016,** *16*, 2077-2126.

(12) Ding, L.; Liu, L.-H.; Shi, Q.; Sun, Y.-Q.; Wang, Y.-J.; Chen, Y.-P. Luminescent 3D Lanthanide–Cadmium Heterometal–Organic Frameworks with Chemical Stability and Selective Luminescent Sensing. *Inorg. Chem.* **2017,** *56*, 14850-14858.

(13) Zhang, S.; Li, H.; Duan, E.; Han, Z.; Li, L.; Tang, J.; Shi, W.; Cheng, P. A 3D Heterometallic Coordination Polymer Constructed by Trimeric {$NiDy_2$} Single-Molecule Magnet Units. *Inorg. Chem.* **2016,** *55*, 1202-1207.

(14) Zheng, B.; Luo, X.; Wang, Z.; Zhang, S.; Yun, R.; Huang, L.; Zeng, W.; Liu, W. An unprecedented water stable acylamide-functionalized metal–organic framework for highly efficient CH_4/CO_2 gas storage/separation and acid–base cooperative catalytic activity. *Inorg. Chem. Front.* **2018,** *5*, 2355-2363.

(15) Li, F. L.; Shao, Q.; Huang, X.; Lang, J. P. Nanoscale Trimetallic Metal-Organic Frameworks Enable Efficient Oxygen Evolution Electrocatalysis. *Angew. Chem. Int. Ed.* **2017,** *57*, 1888-1892.

(16) Zhang, S.; Cheng, P. Recent advances in the construction of lanthanide-copper heterometallic metal-organic frameworks. *CrystEngComm* **2015,** *17*, 4250-4271.

(17) Xie, W.; He, W. W.; Li, S. L.; Shao, K. Z.; Su, Z. M.; Lan, Y. Q. An Anionic Interpenetrated Zeolite-Like Metal-Organic Framework Composite As a Tunable Dual-Emission Luminescent Switch for Detecting Volatile Organic Molecules. *Chem. Eur. J.* **2016,** *22*, 17298-17304.

(18) Yi, F.-Y.; Li, J.-P.; Wu, D.; Sun, Z.-M. A Series of Multifunctional Metal-Organic Frameworks Showing Excellent Luminescent Sensing, Sensitization, and Adsorbent Abilities. *Chem. Eur. J.* **2015,** *21*, 11475-11482.

(19) Yang, Y.; Qiu, F.; Xu, C.; Feng, Y.; Zhang, G.; Liu, W. A multifunctional Eu-CP as a recyclable luminescent probe for the highly sensitive detection of Fe^{3+}/Fe^{2+}, $Cr_2O_7^{2-}$, and nitroaromatic explosives. *Dalton Trans.* **2018,** *47*, 7480-7486.

(20) Zheng, H.-Q.; Liu, C.-Y.; Zeng, X.-Y.; Chen, J.; Lü, J.; Lin, R.-G.; Cao, R.; Lin, Z.-J.; Su, J.-W. MOF-808: A Metal–Organic Framework with Intrinsic Peroxidase-Like Catalytic Activity at Neutral pH for Colorimetric Biosensing. *Inorg. Chem.* **2018,** *57*, 9096-9104.

(21) Chen, S.; Shi, Z.; Qin, L.; Jia, H.; Zheng, H. Two New Luminescent Cd(II)-Metal-Organic Frameworks as Bifunctional Chemosensors for Detection of Cations Fe^{3+}, Anions CrO_4^{2-}, and $Cr_2O_7^{2-}$ in Aqueous Solution. *Cryst. Growth Des.* **2017,** *17*, 67-72.

(22) Liu, L.-H.; Qiu, X.-T.; Wang, Y.-J.; Shi, Q.; Sun, Y.-Q.; Chen, Y.-P. NIR emission and luminescent sensing of a lanthanide–organic framework with Lewis basic imidazole and pyridyl sites. *Dalton Trans.* **2017,** *46*, 12106-12113.

(23) Xie, Y.; Ning, S.; Zhang, Y.; Tang, Z.; Zhang, S.; Tang, R. A 3D supramolecular network as highly selective and sensitive luminescent sensor for PO_4^{3-} and Cu^{2+} ions in aqueous media. *Dyes Pigm.* **2018,** *150*, 36-43.

(24) Zou, J.-Y.; Li, L.; You, S.-Y.; Cui, H.-M.; Liu, Y.-W.; Chen, K.-H.; Chen, Y.-H.; Cui, J.-Z.; Zhang, S.-W. Sensitive luminescent probes of aniline, benzaldehyde and Cr(VI) based on a zinc(II) metal-organic framework and its lanthanide(III) post-functionalizations. *Dyes Pigm.* **2018,** *159*, 429-438.

(25) Wang, Y.; Xu, P.; Xie, Q.; Ma, Q.-Q.; Meng, Y.-H.; Wang, Z.-W.; Zhang, S.; Zhao, X.-J.; Chen, J.; Wang, Z.-L. Cadmium(II)–Triazole Framework as a Luminescent Probe for Ca^{2+} and Cyano Complexes. *Chem. Eur. J.* **2016,** *22*, 10459-10474.

(26) Gu, T.-Y.; Dai, M.; Young, D. J.; Ren, Z.-G.; Lang, J.-P. Luminescent Zn(II) Coordination Polymers for Highly Selective Sensing of Cr(III) and Cr(VI) in Water. *Inorg. Chem.* **2017,** *56*, 4668-4678.

(27) Lu, Y.; Yan, B.; Liu, J.-L. Nanoscale metal-organic frameworks as highly sensitive luminescent sensors for Fe^{2+} in aqueous solution and living cells. *Chem. Commun.* **2014,** *50*, 9969-9972.

(28) Lin, Y.; Zhang, X.; Chen, W.; Shi, W.; Cheng, P. Three Cadmium Coordination Polymers with Carboxylate and Pyridine Mixed Ligands: Luminescent Sensors for Fe^{III} and Cr^{VI} Ions in an Aqueous Medium. *Inorg. Chem.* **2017,** *56*, 11768-11778.

(29) Guo, M.; Sun, Z.-M. Solvents control over the degree of interpenetration in metal-organic frameworks and their high sensitivities for detecting nitrobenzene at ppm level. *J. Mater. Chem.* **2012,** *22*, 15939-15946.

(30) Gao, R.-C.; Guo, F.-S.; Bai, N.-N.; Wu, Y.-L.; Yang, F.; Liang, J.-Y.; Li, Z.-J.; Wang, Y.-Y. Two 3D Isostructural Ln(III)-MOFs: Displaying the Slow Magnetic Relaxation and Luminescence Properties in Detection of Nitrobenzene and $Cr_2O_7^{2-}$. *Inorg. Chem.* **2016,** *55*, 11323-11330.

(31) Lin, Z.-J.; Zheng, H.-Q.; Zheng, H.-Y.; Lin, L.-P.; Xin, Q.; Cao, R. Efficient Capture and Effective Sensing of $Cr_2O_7^{2-}$ from Water Using a Zirconium Metal–Organic Framework. *Inorg. Chem.* **2017,** *56*, 14178-14188.

(32) Lan, A.; Li, K.; Wu, H.; Olson, D. H.; Emge, T. J.; Ki, W.; Hong, M.; Li, J. A Luminescent Microporous Metal-Organic Framework for the Fast and Reversible Detection of High Explosives. *Angew. Chem. Int. Ed.* **2009,** *48*, 2334-2338.

(33) Chen, M.-M.; Zhou, X.; Li, H.-X.; Yang, X.-X.; Lang, J.-P. Luminescent Two-Dimensional Coordination Polymer for Selective and Recyclable Sensing of Nitroaromatic Compounds with High Sensitivity in Water. *Cryst. Growth Des.* **2015,** *15*, 2753-2760.

(34) Jia, X.-X.; Yao, R.-X.; Zhang, F.-Q.; Zhang, X.-M. A Fluorescent Anionic MOF with $Zn_4(trz)_2$ Chain for Highly Selective Visual Sensing of Contaminants: Cr(III) Ion and TNP. *Inorg. Chem.* **2017,** *56*, 2690-2696.

(35) Song, B.-Q.; Qin, C.; Zhang, Y.-T.; Wu, X.-S.; Yang, L.; Shao, K.-Z.; Su, Z.-M. Spontaneous chiral resolution of a rare 3D self-penetration coordination polymer for sensitive aqueous-phase detection of picric acid. *Dalton Trans.* **2015,** *44*, 18386-18394.

(36) Sun, Z.; Li, Y.; Ma, Y.; Li, L. Dual-functional recyclable luminescent sensors based on 2D lanthanide-based metal-organic frameworks for highly sensitive detection of Fe^{3+} and 2,4-dinitrophenol. *Dyes Pigm.* **2017,** *146*, 263-271.

(37) Fu, R.; Hu, S.; Wu, X. Rapid and sensitive detection of nitroaromatic explosives by using new 3D lanthanide phosphonates. *J. Mater. Chem. A* **2017,** *5*, 1952-1956.

(38) Wang, X.-S.; Li, L.; Yuan, D.-Q.; Huang, Y.-B.; Cao, R. Fast, highly selective and sensitive anionic metal-organic framework with nitrogen-rich sites fluorescent chemosensor for nitro explosives detection. *J. Hazard. Mater.* **2018,** *344*, 283-290.

(39) Ji, N.-N.; Shi, Z.-Q.; Hu, H.-L.; Zheng, H.-G. A triphenylamine-functionalized luminescent sensor for efficient p-nitroaniline detection. *Dalton Trans.* **2018,** *47*, 7222-7228.

(40) Gong, W.-J.; Ren, Z.-G.; Li, H.-X.; Zhang, J.-G.; Lang, J.-P. Cadmium(II) Coordination Polymers of 4-Pyr-poly-2-ene and Carboxylates: Construction, Structure, and Photochemical Double [2 + 2] Cycloaddition and Luminescent Sensing of Nitroaromatics and Mercury(II) Ions. *Cryst. Growth Des.* **2017,** *17*, 870-881.

(41) Nagarkar, S. S.; Desai, A. V.; Ghosh, S. K. A fluorescent metal-organic framework for highly selective detection of nitro explosives in the aqueous phase. *Chem. Commun.* **2014,** *50*, 8915-8918.

(42) Hu, Y.; Ding, M.; Liu, X.-Q.; Sun, L.-B.; Jiang, H.-L. Rational synthesis of an exceptionally stable Zn(ii) metal–organic framework for the highly selective and sensitive detection of picric acid. *Chem. Commun.* **2016,** *52*, 5734-5737.

(43) Wu, Z.-F.; Huang, X.-Y. A series of Mg-Zn heterometallic coordination polymers: synthesis, characterization, and fluorescence sensing for Fe^{3+}, CS_2, and nitroaromatic compounds. *Dalton Trans.* **2017,** *46*, 12597-12604.

(44) Nagarkar, S. S.; Desai, A. V.; Samanta, P.; Ghosh, S. K. Aqueous phase selective detection of 2,4,6-trinitrophenol using a fluorescent metal-organic framework with a pendant recognition site. *Dalton Trans.* **2015,** *44*, 15175-15180.

(45) Zhang, C.; Yan, Y.; Sun, L.; Liang, Z.; Li, J. Solvent-induced construction of two zinc metal-organic frameworks for highly selective detection of nitroaromatic explosives. *CrystEngComm* **2016,** *18*, 4102-4108.

(46) Yang, Y.; Song, X.; Xu, C.; Wang, Y.; Zhang, G.; Liu, W. A multifunctional and recyclable terbium(III) coordination polymer: displaying highly selective and sensitive detection of Fe^{3+} and Cr^{VI} anions, and picric acid in aqueous media. *Dalton Trans.* **2018,** *47*, 11077-11083.

(47) Wang, B.; Lv, X.-L.; Feng, D.; Xie, L.-H.; Zhang, J.; Li, M.; Xie, Y.; Li, J.-R.; Zhou, H.-C. Highly Stable Zr(IV)- Based Metal-Organic Frameworks for the Detection and Removal of Antibiotics and Organic Explosives in Water. *J. Am. Chem. Soc.* **2016,** *138*, 6204-6216.

(48) Joarder, B.; Desai, A. V.; Samanta, P.; Mukherjee, S.; Ghosh, S. K. Selective and Sensitive Aqueous-Phase Detection of 2,4,6-Trinitrophenol (TNP) by an Amine-Functionalized Metal-Organic Framework. *Chem. Eur. J.* **2014,** *21*, 965-969.

(49) Yao, R.-X.; Cui, X.; Jia, X.-X.; Zhang, F.-Q.; Zhang, X.-M. A Luminescent Zinc(II) Metal-Organic Framework (MOF) with Conjugated π-Electron Ligand for High Iodine Capture and Nitro-Explosive Detection. *Inorg. Chem.* **2016,** *55*, 9270-9275.

(50) Mukherjee, S.; Desai, A. V.; Manna, B.; Inamdar, A. I.; Ghosh, S. K. Exploitation of Guest Accessible Aliphatic Amine Functionality of a Metal-Organic Framework for Selective Detection of 2,4,6-Trinitrophenol (TNP) in Water. *Cryst. Growth Des.* **2015,** *15*, 4627-4634.

(51) Das, D.; Biradha, K. Luminescent Coordination Polymers of Naphthalene Based Diamide with Rigid and Flexible Dicarboxylates: Sensing of Nitro Explosives, Fe(III) Ion, and Dyes. *Cryst. Growth Des.* **2018,** *18*, 3683-3692.

(52) Chen, D.-M.; Tian, J.-Y.; Wang, Z.-W.; Liu, C.-S.; Chen, M.; Du, M. An anionic Na(I)-organic framework platform: separation of organic dyes and post-modification for highly sensitive detection of picric acid. *Chem. Commun.* **2017,** *53*, 10668-10671.

(53) Luo, X.; Zhang, X.; Duan, Y.; Wang, X.; Zhao, J. A novel luminescent Pb(II) - organic framework exhibiting a rapid and selective detection of trace amounts of NACs and Fe^{3+} with excellent recyclability. *Dalton Trans.* **2017,** *46*, 6303-6311.

(54) Song, J. H.; Kim, Y.; Lim, K. S.; Kang, D. W.; Lee, W. R.; Hong, C. S. Phase Transformation, Exceptional Quenching Efficiency, and Discriminative Recognition of Nitroaromatic Analytes in Hydrophobic, Nonporous Zn(II) Coordination Frameworks. *Inorg. Chem.* **2017,** *56*, 305-312.

(55) Dolomanov, O. V.; Bourhis, L. J.; Gildea, R. J.; Howard, J. A. K.; Puschmann, H. OLEX2: a complete structure solution, refinement and analysis program. *J. Appl. Crystallogr.* **2009,** *42*, 339-341.

(56) Sheldrick, G. Crystal structure refinement with SHELXL. *Acta Crystallogr., Sect. C: Struct. Chem.* **2015,** *71*, 3-8.

(57) Blatov, V. A.; Shevchenko, A. P.; Proserpio, D. M. Applied Topological Analysis of Crystal Structures with the Program Package ToposPro. *Cryst. Growth Des.* **2014,** *14*, 3576-3586. TOPOS software available at http://topospro.com.

(58) Zhang, S.; Ma, J.; Zhang, X.; Duan, E.; Cheng, P. Assembly of Metal-Organic Frameworks Based on 3,3′,5,5′-Azobenzene-tetracarboxylic Acid: Photoluminescences, Magnetic Properties, and Gas Separations. *Inorg. Chem.* **2015,** *54*, 586-595.

(59) Ning, S.; Chen, H.; Zhang, S.; Cheng, P. A 2D water-stable metal–organic framework for fluorescent detection of nitroaromatics. *Polyhedron* **2018,** *155*, 457-463.

(60) Analytical Methods, C. Recommendations for the definition, estimation and use of the detection limit. *Analyst* **1987,** *112*, 199-204.

For Table of Contents Use Only

A Functional 2D Coordination Polymer Exhibiting Luminescent Detection of Nitroaromatics

Zilong Tang, Hongjuan Chen, Yong Zhang, Baishu Zheng, Shaowei Zhang, and Peng Cheng**

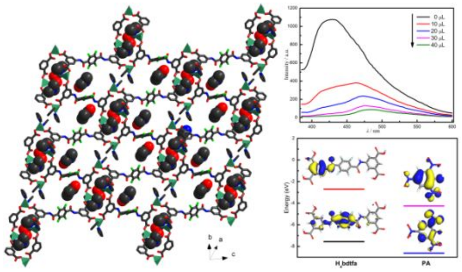

A new polyfluorinated-aromatic carboxylic acid was designed and used to construct luminescent coordination polymer, which can serve as a highly sensitive sensor for detecting nitroaromatic compounds.